

Simplified Matrix Calculation for Analysis of Girder-Deck Bridge Systems

Alvaro Gaute-Alonso and David Garcia-Sanchez

Abstract

In the design of girder-deck bridge systems, it is necessary to determine the cross-sectional distribution of live loads between the different beams that make up the cross section of the deck. This article introduces a novel method that allows calculating the cross-sectional distribution of live loads on beam decks by applying a matrix formulation that reduces the structural problem to 2 degrees of freedom for each beam: the deflection and the rotation of the deck slab at the center of the beam's span. To demonstrate the proposed method, the procedures are given through three different examples by applying loads to a bridge model. Deflection, bending moment, and shear force of the bridge girders are calculated and discussed through the given examples. The use of the proposed novel method of analysis will result in significant savings in material resources and computing time and contributes in the minimization of total costs, and it contributes in the smart modeling process for girder bridge behavior analysis allowing to feed a bridge digital twin (DT) model based on Inverse Modeling holding the latest updated information provided by distributed sensors. The presented methodology contributes also to speed up real-time decision support system (DSS) demands.

Keywords: cross-sectional load distribution, girder bridge decks, optimized matrix method, load distribution factors, structural grillage models

1. Introduction

Girder bridge decks are a structural typology commonly used in the design of road and railway bridges, and therefore, any optimization in their calculation has a depth impact on the project phase. As explained in [1], the design process relies solely on the designers' experience, intuition, and ingenuity resulting in a depth cost material, time, and human effort. It is very common to use structural grillage models [2–10] to calculate the cross-sectional distribution of live loads between the different beams that make up the cross section of the deck. Another way to deal with the design and calculation of such decks would be to apply different formulations contained in the bridge design standards that allow approximating the cross-sectional distribution of the bending moment and shear stress caused by live loads through what is known as

the load distribution factor “LDF” [11–23]. The “LDF” associated with each case study is conditioned by the type and number of beams, their spacing and length, as well as the existence or not of transverse diaphragms that bring transverse rigidity to the deck.

However, the LDF does not allow determining the distribution of bending stresses on all beams; therefore, the design is oversized. The need for a method to calculate the cross-sectional distribution across all types of beams, without resorting to complex structural grillage models or finite element models in specific structure calculation programs, or to approximate parametric methods based on the “LDF,” is one of the authors’ motivations for the development of the research work that has given rise to this article.

2. Traditional methods for girder bridge deck analysis

Structural grillage models began to be used for the analysis of cross-sectional distribution on beams in the 1960s. These models divide the beam deck into longitudinal and transverse beams (**Figure 1**). Longitudinal beams are responsible for providing the longitudinal bending stiffness of the deck, considering as many longitudinal beams as beams conform to the analyzed beam deck. The structural section of each of the longitudinal beams shall be the result of the section composed of the beam analyzed and the effective depth of the contributing deck with that beam [24, 25]. The cross-sectional distribution of the structural model is provided by the cross-beams and the torsional stiffness of the longitudinal beams. The structural section of the cross-beams corresponds to a rectangular section with an equivalent depth to the slab thickness and a depth according to the discretization used in the grillage models. The analysis of such structural models involves the use of specific structure calculation programs that provide the computing power necessary for the resolution of the proposed matrix problem.

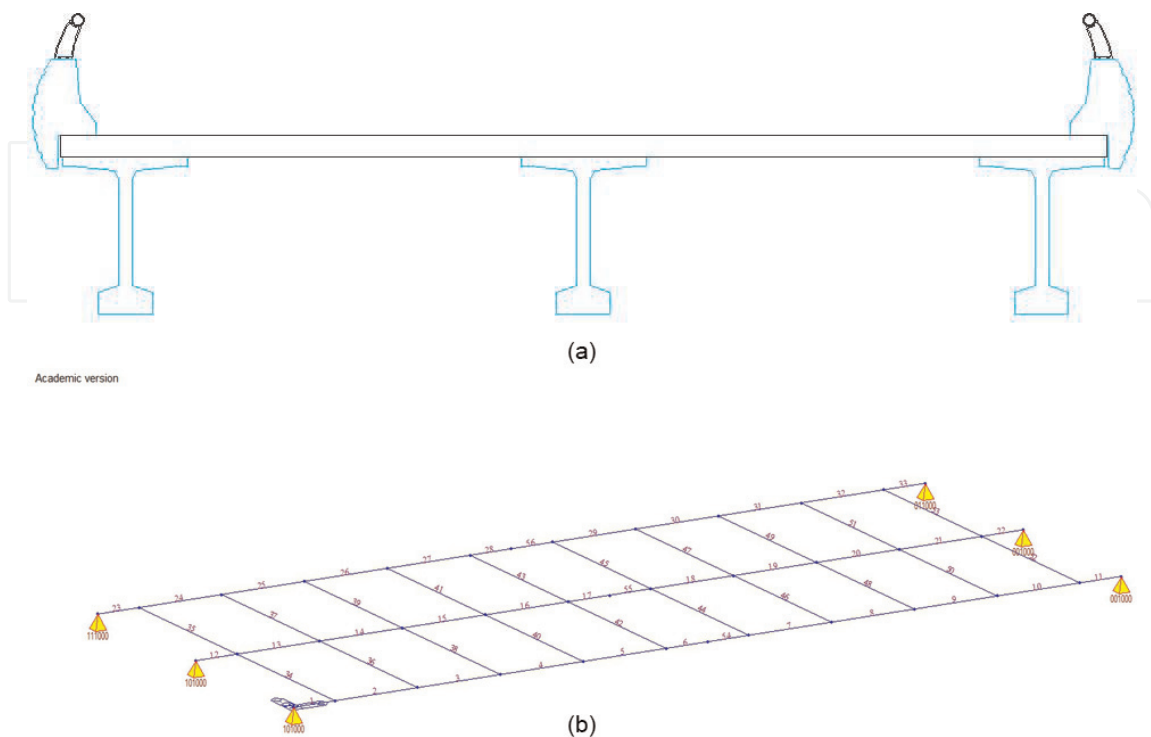


Figure 1.
Grillage discretization: (a) girder bridge deck cross section; (b) structural grillage model.

The use of structural grillage models allows obtaining the structural response of girder bridge decks to live loads, adequately manifesting the cross-sectional distortion of the girder bridge deck and the distribution of stresses on each of the longitudinal beams that make up the deck. However, such models involve complex, time-consuming analysis that involves the need to use specific structure calculation programs, making it necessary to use simplified methods for the start of the design process.

The concept of LDF was first introduced using empirical formulas at the American Association of State Depthway Officials (AASHTO) in 1931 [26]; these methods propose calculating the cross-sectional distribution on beam bridge decks roughly. The LDF is calculated from a series of formulations that parametrically treat the calculation of the percentage of bending moment and shear stress supported by the most requested longitudinal beam. The parameters that condition the calculation of the LDF are the depth of the beam, the span length, the spacing, the number of beams, the position of the load, and the beam position. This method provides an approximate value of the maximum bending stresses on the beams but is not able to reproduce the cross-sectional distribution of longitudinal bending between all the beams that make up the deck.

3. Proposed method for the study of the cross-sectional load distribution on a girder bridge deck

The authors propose the use of a method that allows obtaining the cross-sectional distribution of live loads on girder bridge decks without using empirical formulas of LDFs or complex structural models involving the use of specific structure calculation programs. The proposed method is based on using a virtual model that reflects the transverse stiffness of the slab deck, supported on a series of springs that provide the flexural stiffness Eq. (1) and torsional stiffness Eq. (2) of the longitudinal beams that make up the girder bridge deck (**Figure 2**).

$$K_{v,i} = \frac{48 \cdot EI_i}{L^3} \tag{1}$$

$$K_{t,i} = \frac{2 \cdot GJ_i}{L} \tag{2}$$

where EI_i = longitudinal bending stiffness of beam “i”; GJ_i = longitudinal torsional stiffness of beam “i”; L = distance between bridge supports.

The proposed method considers 2 degrees of freedom for each longitudinal beam on the bridge deck: (1) the deflection and (2) the rotation of the deck slab at the center of the beam’s span. **Figure 2** represents the structural model scheme for a girder

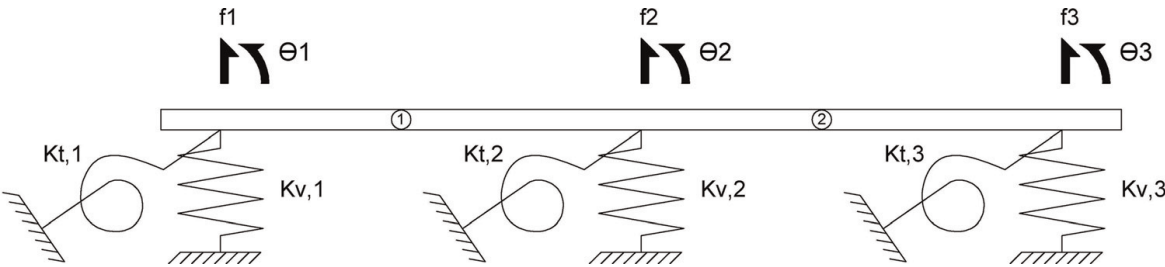


Figure 2.
Proposed method model for cross-sectional distribution on a girder bridge deck.

bridge deck composed of three longitudinal beams. The matrix approach that solves the structural problem of the cross-sectional distribution of live loads between the different beams that make up the deck is raised in matrix Eqs. (3), (4), (5). The stiffness of the springs that represents the longitudinal bending and the torsional stiffness of the longitudinal beams that make up the model corresponds to the stiffness equivalent to the center of the span.

$$K_e = \frac{EI_e}{L_e^3} \begin{pmatrix} 12 & 6L_e & -12 & 6L_e \\ 6L_e & 4L_e^2 & -6L_e & 2L_e^2 \\ -12 & -6L_e & 12 & -6L_e \\ 6L_e & 2L_e^2 & -6L_e & 4L_e^2 \end{pmatrix} = \begin{pmatrix} K_{11,e} & K_{12,e} \\ K_{21,e} & K_{22,e} \end{pmatrix} \quad (3)$$

$$K_{Bi} = \begin{pmatrix} k_{v,i} & 0 \\ 0 & k_{t,i} \end{pmatrix} \quad (4)$$

$$\begin{pmatrix} P_1 \\ M_{t,1} \\ P_2 \\ M_{t,2} \\ P_3 \\ M_{t,3} \end{pmatrix} = \begin{pmatrix} K_{11,1} + K_{B1} & K_{12,1} & 0 & 0 \\ K_{21,1} & K_{22,1} + K_{11,2} + K_{B2} & 0 & 0 \\ 0 & 0 & K_{12,2} & 0 \\ 0 & 0 & K_{21,2} & K_{22,2} + K_{B3} \end{pmatrix} \times \begin{pmatrix} f_{v,1} \\ \theta_1 \\ f_{v,2} \\ \theta_2 \\ f_{v,3} \\ \theta_3 \end{pmatrix} \quad (5)$$

Where EI_e = transverse bending stiffness of element “e” of the upper deck slab; L_e = length of element “e” of the upper deck slab; $f_{v,i}$ = vertical displacement experienced by longitudinal beam “i”; θ_i = transverse rotation of the bridge deck over the longitudinal beam “i.”

3.1 Loads applied in the center of the span of the longitudinal beams

The maximum longitudinal bending stress in each of the longitudinal beams that make up the bridge deck corresponds to the application of a point load in the center of the beam span. The distribution of the maximum bending moment and maximum shear stress in the different longitudinal beams is obtained by Eqs. (6) and (7), respectively.

$$M_{f\dot{m}ax,n} = \frac{Q \cdot L}{4} \cdot \frac{f_{v,n}}{\sum_{i=1}^N f_{v,i}} \quad (6)$$

$$Q_{\dot{m}ax,n} = \frac{Q \cdot L}{2} \cdot \frac{f_{v,n}}{\sum_{i=1}^N f_{v,i}} \quad (7)$$

where Q = point load value; L = girder bridge span length.

Example 3.1.1.

In the study of the structural behavior of the bridge deck represented in **Figure 3**, it is desired to know the distribution of the bending moment and the shear force in each of the longitudinal beams generated by the application of the following load states: (a) a point load of 300 kN in the center of the span of beam 1, and (b) a point

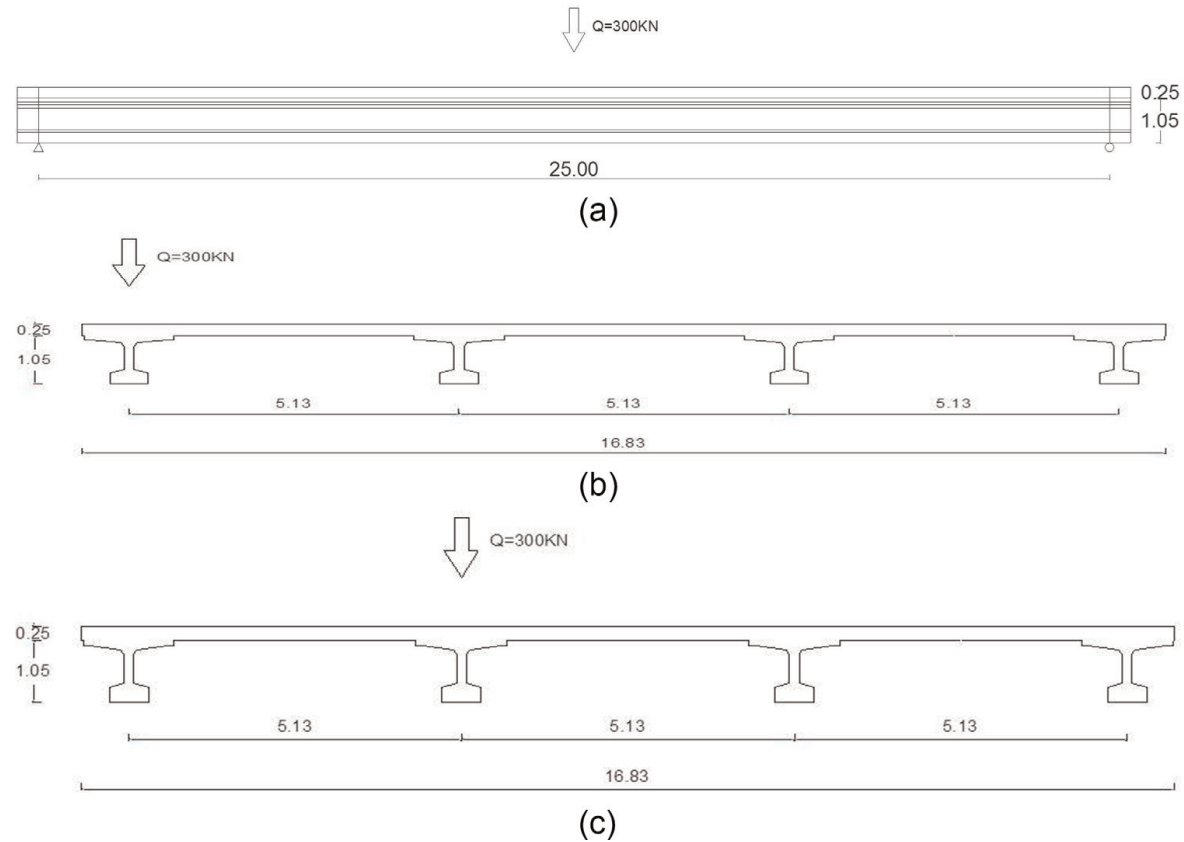


Figure 3.
Girder bridge deck: (a) side view of load states 1 and 2; (b) front view of load state 1; (c) front view of load state 2.

load of 300 kN in the center of the span of beam 2. The girder bridge is made up of four longitudinal beams 1.05 meters deep (two end beams and two central beams) and an upper slab 0.25 meters thick and 16.83 meters wide. Considering the effective width of the upper slab in each of the longitudinal beams, the inertia to the longitudinal bending of the end and central beams takes the value of 0.1445 m^4 and 0.1904 m^4 , respectively. The longitudinal torsional inertia of the longitudinal beams takes the value of $4.3 \cdot 10^{-3} \text{ m}^4$. The spacing between longitudinal beams is 5.13 meters, while the distance between the support devices of each longitudinal beam is 25 meters. Both the upper slab and the longitudinal beams are made of structural concrete whose modulus of elasticity reaches 35,000 MPa.

The stiffness of the springs on which the upper slab of the bridge deck rests, and which simulates the bending and torsional stiffness of the longitudinal beams (**Figure 4**), is calculated as follows:

End beams

$$K_{v,end} = \frac{48 \cdot EI_{end}}{L^3} = \frac{48 \cdot 3.5 \cdot 10^7 \text{ KN/m}^2 \cdot 0.1445 \text{ m}^4}{(25 \text{ m})^3} = 15,537 \text{ KN/m}$$

$$K_{t,end} = \frac{2 \cdot GJ_{end}}{L} = \frac{2 \cdot \frac{3.5 \cdot 10^7 \text{ KN/m}^2}{2 \cdot (1+0.2)} \cdot 4.3 \cdot 10^3 \text{ m}^4}{25 \text{ m}} = 5,017 \text{ KN} \cdot \text{m}$$

$$K_{B,end} = \begin{pmatrix} k_{v,end} & 0 \\ 0 & k_{t,end} \end{pmatrix} = \begin{pmatrix} 15,537 \text{ KN/m} & 0 \\ 0 & 5,017 \text{ KN} \cdot \text{m} \end{pmatrix}$$

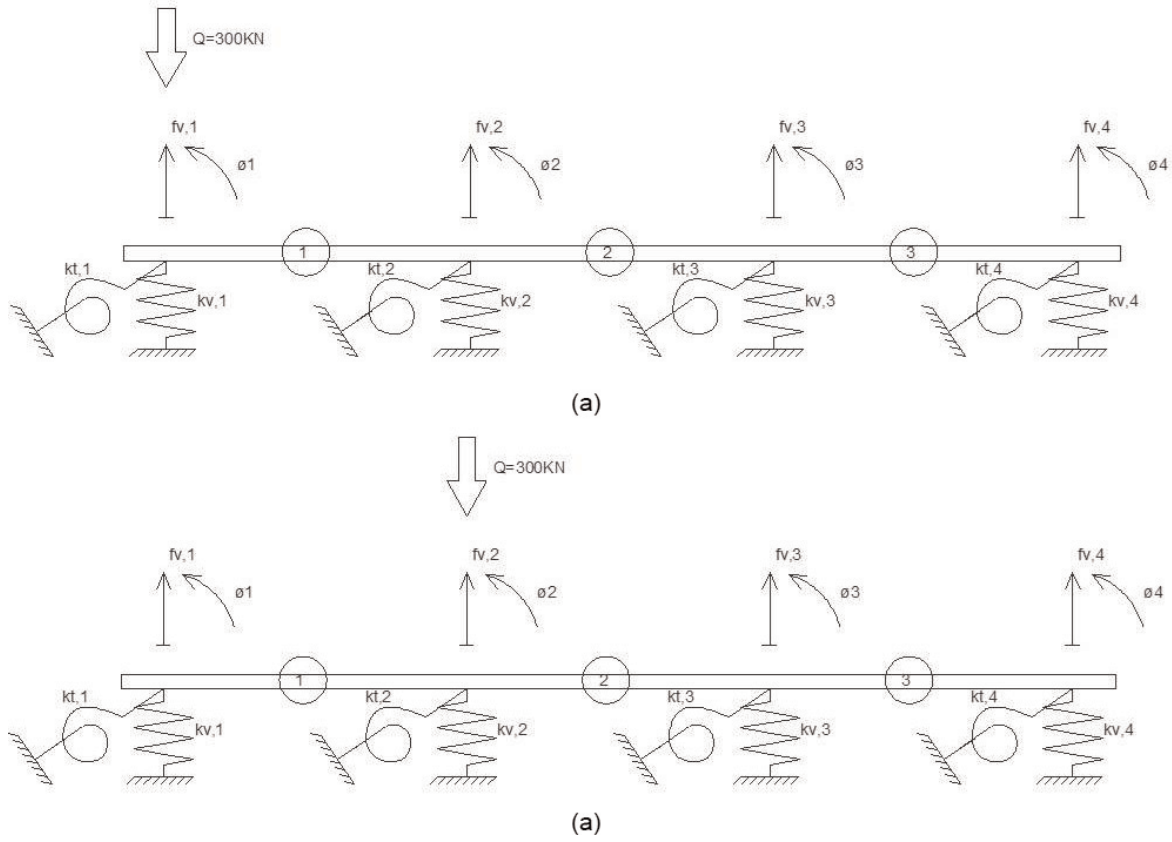


Figure 4.
Proposed structural model: (a) load state 1; (b) load state 2.

Central beams

$$K_{v,c} = \frac{48 \cdot EI_{end}}{L^3} = \frac{48 \cdot 3.5 \cdot 10^7 \text{KN/m}^2 \cdot 0.1904 \text{m}^4}{(25\text{m})^3} = 20,472 \text{KN/m}$$

$$K_{t,c} = \frac{2 \cdot GJ_{end}}{L} = \frac{2 \cdot \frac{3.5 \cdot 10^7 \text{KN/m}^2}{2 \cdot (1+0.2)} \cdot 4.3 \cdot 10^3 \text{m}^4}{25\text{m}} = 5,017 \text{KN} \cdot \text{m}$$

$$K_{B,c} = \begin{pmatrix} k_{v,end} & 0 \\ 0 & k_{t,end} \end{pmatrix} = \begin{pmatrix} 20,472 \text{KN/m} & 0 \\ 0 & 5,017 \text{KN} \cdot \text{m} \end{pmatrix}$$

The mechanical characteristics of the beam elements that simulate the transverse distribution provided by the upper slab (**Figure 4**) are calculated as follows:

$$I = \frac{1}{12} \cdot 20\text{m} \cdot (0.25\text{m})^3 = 2.6 \cdot 10^{-2} \text{m}^4$$

$$L = 5,13 \text{ m}$$

$$K = \frac{E \cdot I}{L^3} \begin{pmatrix} 12 & 6L & -12 & 6L \\ 6L & 4L^2 & -6L & 2L^2 \\ -12 & -6L & 12 & -6L \\ 6L & 2L^2 & -6L & 4L^2 \end{pmatrix}$$

$$K = \begin{pmatrix} 81,020KN/m & 207,800KN & -81,020KN/m & 207,800KN \\ 207,800KN & 710,690KN \cdot m & -207,800KN & 355,340KN \cdot m \\ -81,020KN/m & -207,800KN & 81,020KN/m & -207,800KN \\ 207,800KN & 355,340KN \cdot m & -207,800KN & 710,690KN \cdot m \end{pmatrix}$$

$$K = \begin{pmatrix} K_{11} & K_{12} \\ K_{21} & K_{22} \end{pmatrix}$$

The global stiffness matrix used in the proposed method for the analysis of the transverse distribution of live loads in girder bridge decks is obtained as follows:

$$K_G = \begin{pmatrix} & & & 0 & 0 & 0 & 0 \\ & K_{11} + K_{B,end} & K_{12} & 0 & 0 & 0 & 0 \\ & K_{21} & K_{22} + K_{11} + K_{B,c} & & & 0 & 0 \\ & & & K_{12} & & 0 & 0 \\ 0 & 0 & & & & & \\ & & K_{21} & & & & \\ 0 & 0 & & K_{22} + K_{11} + K_{B,c} & K_{12} & & \\ 0 & 0 & 0 & 0 & & K_{21} & K_{22} + K_{B,end} \\ 0 & 0 & 0 & 0 & & & \end{pmatrix}$$

The transversal distribution of each load state is obtained by planting the compatibility between loads and displacements:

Load state 1

$$\begin{pmatrix} -300KN \\ 0 \\ 0 \\ 0 \\ 0 \\ 0 \\ 0 \\ 0 \end{pmatrix} = \begin{pmatrix} & & & 0 & 0 & 0 & 0 \\ & K_{11} + K_{B,end} & K_{12} & 0 & 0 & 0 & 0 \\ & K_{21} & K_{22} + K_{11} + K_{B,c} & & & 0 & 0 \\ & & & K_{12} & & 0 & 0 \\ 0 & 0 & & & & & \\ & & K_{21} & & & & \\ 0 & 0 & & K_{22} + K_{11} + K_{B,c} & K_{12} & & \\ 0 & 0 & 0 & 0 & & K_{21} & K_{22} + K_{B,end} \\ 0 & 0 & 0 & 0 & & & \end{pmatrix} \times \begin{pmatrix} f_{v,1} \\ \theta_1 \\ f_{v,2} \\ \theta_2 \\ f_{v,3} \\ \theta_3 \\ f_{v,4} \\ \theta_4 \end{pmatrix}$$

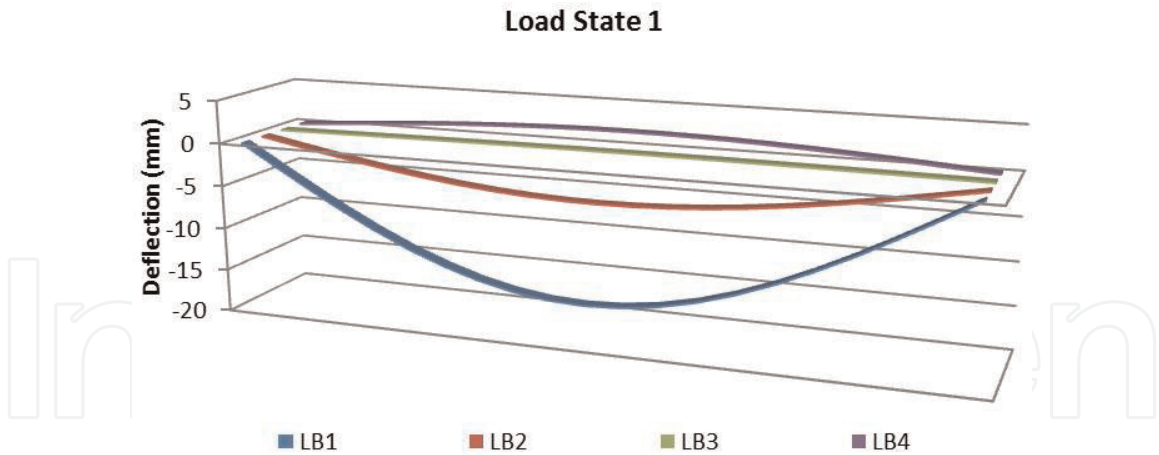


Figure 5.
Deflections of longitudinal beams in load state 1.

Deflections (**Figure 5**) and rotations

$$d = \begin{pmatrix} -15.14 \text{ mm} \\ 2.25 \text{ mRad} \\ -4.75 \text{ mm} \\ 1.55 \text{ mRad} \\ 0.24 \text{ mm} \\ 0.52 \text{ mRad} \\ 1.79 \text{ mm} \\ 0.19 \text{ mRad} \end{pmatrix}$$

Maximum bending moments

$$M_{f\dot{m}ax,n} = \frac{Q \cdot L}{4} \cdot \frac{f_{v,n}}{\sum_{i=1}^N f_{v,i}} = \begin{pmatrix} 1,588 \text{ KN} \cdot \text{m} \\ 499 \text{ KN} \cdot \text{m} \\ -25 \text{ KN} \cdot \text{m} \\ -187 \text{ KN} \cdot \text{m} \end{pmatrix}$$

Maximum shear forces

$$Q_{\dot{m}ax,n} = \frac{Q \cdot L}{2} \cdot \frac{f_{v,n}}{\sum_{i=1}^N f_{v,i}} = \begin{pmatrix} 127 \text{ KN} \\ 40 \text{ KN} \\ -2 \text{ KN} \\ -15 \text{ KN} \end{pmatrix}$$

Load state 2

$$\begin{pmatrix} 0 \\ 0 \\ -300\text{KN} \\ 0 \\ 0 \\ 0 \\ 0 \end{pmatrix} = \begin{pmatrix} 0 & 0 & 0 & 0 \\ K_{11} + K_{B,end} & K_{12} & 0 & 0 \\ K_{21} & K_{22} + K_{11} + K_{B,c} & 0 & 0 \\ & K_{12} & 0 & 0 \\ 0 & 0 & K_{21} & 0 \\ 0 & 0 & K_{22} + K_{11} + K_{B,c} & K_{12} \\ 0 & 0 & K_{21} & K_{22} + K_{B,end} \\ 0 & 0 & 0 & 0 \end{pmatrix} \times \begin{pmatrix} f_{v,1} \\ \theta_1 \\ f_{v,2} \\ \theta_2 \\ f_{v,3} \\ \theta_3 \\ f_{v,4} \\ \theta_4 \end{pmatrix}$$

Deflections (**Figure 6**) and rotations

$$d = \begin{pmatrix} -4.75 \text{ mm} \\ -0.76 \text{ mRad} \\ -7.21 \text{ mm} \\ 0.08 \text{ mRad} \\ -4.01 \text{ mm} \\ 0.87 \text{ mRad} \\ 0.24 \text{ mm} \\ 0.80 \text{ mRad} \end{pmatrix}$$

Maximum bending moments

$$M_{f_{\max,n}} = \frac{Q \cdot L}{4} \cdot \frac{f_{v,n}}{\sum_{i=1}^N f_{v,i}} = \begin{pmatrix} 566 \text{ KN} \cdot \text{m} \\ 859 \text{ KN} \cdot \text{m} \\ 478 \text{ KN} \cdot \text{m} \\ -28 \text{ KN} \cdot \text{m} \end{pmatrix}$$

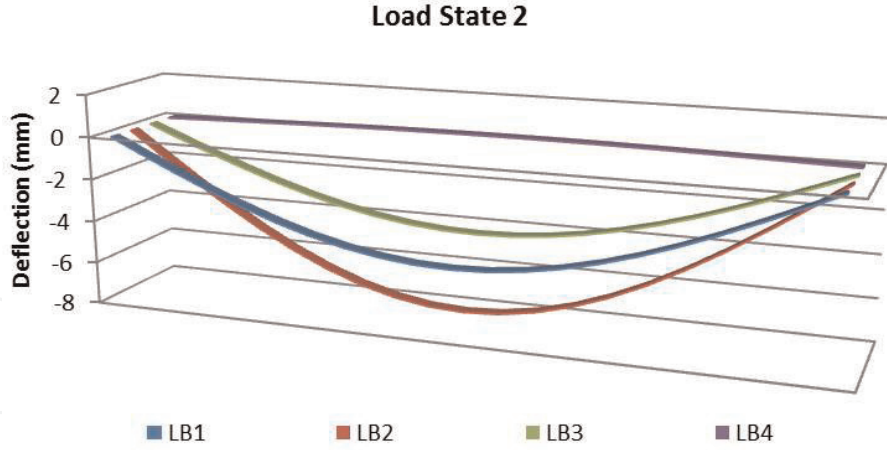


Figure 6.
Deflections of longitudinal beams in load state 2.

Maximum shear forces

$$Q_{\max,n} = \frac{Q \cdot L}{2} \cdot \frac{f_{v,n}}{\sum_{i=1}^N f_{v,i}} = \begin{pmatrix} 45 \text{ KN} \\ 69 \text{ KN} \\ 38 \text{ KN} \\ -2 \text{ KN} \end{pmatrix}$$

3.2 Loads applied at a distance “x” from one of the supports of the longitudinal beams

The proposed method is applicable to calculate the structural response of a girder bridge deck to the application of a vertical load in any cross section. Using the Maxwell-Betti reciprocity theorem [27], for the application of a point load of value “Q” at a distance “x” from one of the two support points of a longitudinal beam, the deflection at the center of the span is obtained by applying the formulation reflected in Eq. (8). Likewise, the distribution of the maximum bending moment and maximum shear stress in the different longitudinal beams is obtained by Eqs. (9) and (10), respectively.

$$f_{cl,Q(x),i} = f_{v,i} \cdot \sin\left(\frac{\pi \cdot x}{L}\right) \quad (8)$$

$$M_{f\max,n} = \frac{Q \cdot (L - x) \cdot x}{L} \cdot \frac{f_{v,n}}{\sum_{i=1}^N f_{v,i}} \quad / \quad x \leq L/2 \quad (9)$$

$$Q_{n\max,n} = \frac{Q \cdot (L - x)}{L} \cdot \frac{f_{v,n}}{\sum_{i=1}^N f_{v,i}} \quad / \quad x \leq L/2 \quad (10)$$

Example 3.2.1.

In the study of the structural behavior of the bridge deck analyzed in Example 3.1.1., it is intended to know the deflection in the center of the span of the longitudinal beams, as well as the distribution of the maximum bending moment and the maximum shear force in each of the longitudinal beams generated by the application of the following load states: (a) a point load of 300 kN at a distance equivalent to L/3 from



Figure 7.
 Point load of 300 kN at a distance equivalent to L/3 from one of the supports of a beam.

one of the supports of beam 1, and (b) a point load of 300 kN at a distance equivalent to L/3 from one of the supports of beam 2 (**Figure 7**).

Load state 1

Deflection in the center of the spam of the longitudinal beams

$$f_{cl,Q(x),i} = f_{v,i} \cdot \sin\left(\frac{\pi \cdot x}{L}\right) = \begin{pmatrix} -13.12 \text{ mm} \\ -4.12 \text{ mm} \\ 0.20 \text{ mm} \\ 1,55 \text{ mm} \end{pmatrix}$$

Maximum bending moments

$$M_{f\acute{m}ax,n} = \frac{Q \cdot (L - x) \cdot x}{L} \cdot \frac{f_{v,n}}{\sum_{i=1}^N f_{v,i}} = \begin{pmatrix} 1,412 \text{ kN} \cdot \text{m} \\ 443 \text{ kN} \cdot \text{m} \\ -22 \text{ kN} \cdot \text{m} \\ -167 \text{ kN} \cdot \text{m} \end{pmatrix}$$

Maximum shear forces

$$Q_{\acute{m}ax,n} = \frac{Q \cdot (L - x)}{L} \cdot \frac{f_{v,n}}{\sum_{i=1}^N f_{v,i}} = \begin{pmatrix} 169 \text{ kN} \\ 53 \text{ kN} \\ -3 \text{ kN} \\ -20 \text{ kN} \end{pmatrix}$$

Load state 1

Deflection in the center of the spam of the longitudinal beams

$$f_{cl,Q(x),i} = f_{v,i} \cdot \sin\left(\frac{\pi \cdot x}{L}\right) = \begin{pmatrix} -4.12 \text{ mm} \\ -6.25 \text{ mm} \\ -3.48 \text{ mm} \\ 0.20 \text{ mm} \end{pmatrix}$$

Maximum bending moments

$$M_{f\acute{m}ax,n} = \frac{Q \cdot (L - x) \cdot x}{L} \cdot \frac{f_{v,n}}{\sum_{i=1}^N f_{v,i}} = \begin{pmatrix} 503 \text{ kN} \cdot \text{m} \\ 764 \text{ kN} \cdot \text{m} \\ 425 \text{ kN} \cdot \text{m} \\ -25 \text{ kN} \cdot \text{m} \end{pmatrix}$$

Maximum shear forces

$$Q_{max,n} = \frac{Q \cdot (L - x)}{L} \cdot \frac{f_{v,n}}{\sum_{i=1}^N f_{v,i}} = \begin{pmatrix} 60 \text{ KN} \\ 92 \text{ KN} \\ 51 \text{ KN} \\ -3 \text{ KN} \end{pmatrix}$$

3.3 Loads applied at any point on the bridge deck

The proposed method is applicable to calculate the transverse response of girder bridge decks to the application of a vertical load at any point of the cross section. As in any matrix calculation, if the vertical load acts on a section of slab between longitudinal beams, the degrees of freedom of the structural model are locked and the reactions in the locked degrees of freedom are calculated (rigid step). Subsequently, the degrees of freedom are released and loaded with the reactions obtained in the previous step to obtain the vertical displacement of each of the longitudinal beams that make up the bridge deck (flexible step).

Example 3.3.1.

In the study of the structural behavior of the bridge deck analyzed in Example 3.1.1., it is intended to know the deflection in the center of the span of the longitudinal beams, as well as the distribution of the maximum bending moment and the maximum shear force in each of the longitudinal beams generated by the application of the load states described in **Figure 8**.

Rigid step (**Figure 9**).

The load generated by the action of the truck axles on longitudinal beams 1 and 2 is obtained considering the compatibility between loads and movements in the upper slab between longitudinal beams 1 and 2.

$$\begin{pmatrix} V_{LB1} \\ M_{LB1} \\ -Q_i \\ 0 \\ -Q_i \\ 0 \\ V_{LB2} \\ M_{LB2} \end{pmatrix} = \begin{pmatrix} & & & 0 & 0 & 0 & 0 \\ K_{11,1} & K_{12,1} & & 0 & 0 & 0 & 0 \\ K_{21,1} & K_{22,1} + K_{11,2} & & & 0 & 0 & \\ & K_{12,2} & & 0 & 0 & & \\ 0 & 0 & K_{21,2} & & & & \\ 0 & 0 & & K_{22,2} + K_{11,3} & -K_{12,3} & & \\ 0 & 0 & 0 & 0 & K_{21,3} & K_{22,3} & \\ 0 & 0 & 0 & 0 & & & \end{pmatrix} \cdot \begin{pmatrix} 0 \\ 0 \\ v2 \\ \theta2 \\ v3 \\ \theta3 \\ 0 \\ 0 \end{pmatrix}$$

Load on longitudinal beams 1 and 2

$$Q = \begin{pmatrix} 1.46 \cdot Q \text{ KN} \\ 1.09 \cdot Q \text{ KN} \cdot m \\ 0.54 \cdot Q \text{ KN} \\ -0.70 \cdot Q \text{ KN} \cdot m \end{pmatrix}$$

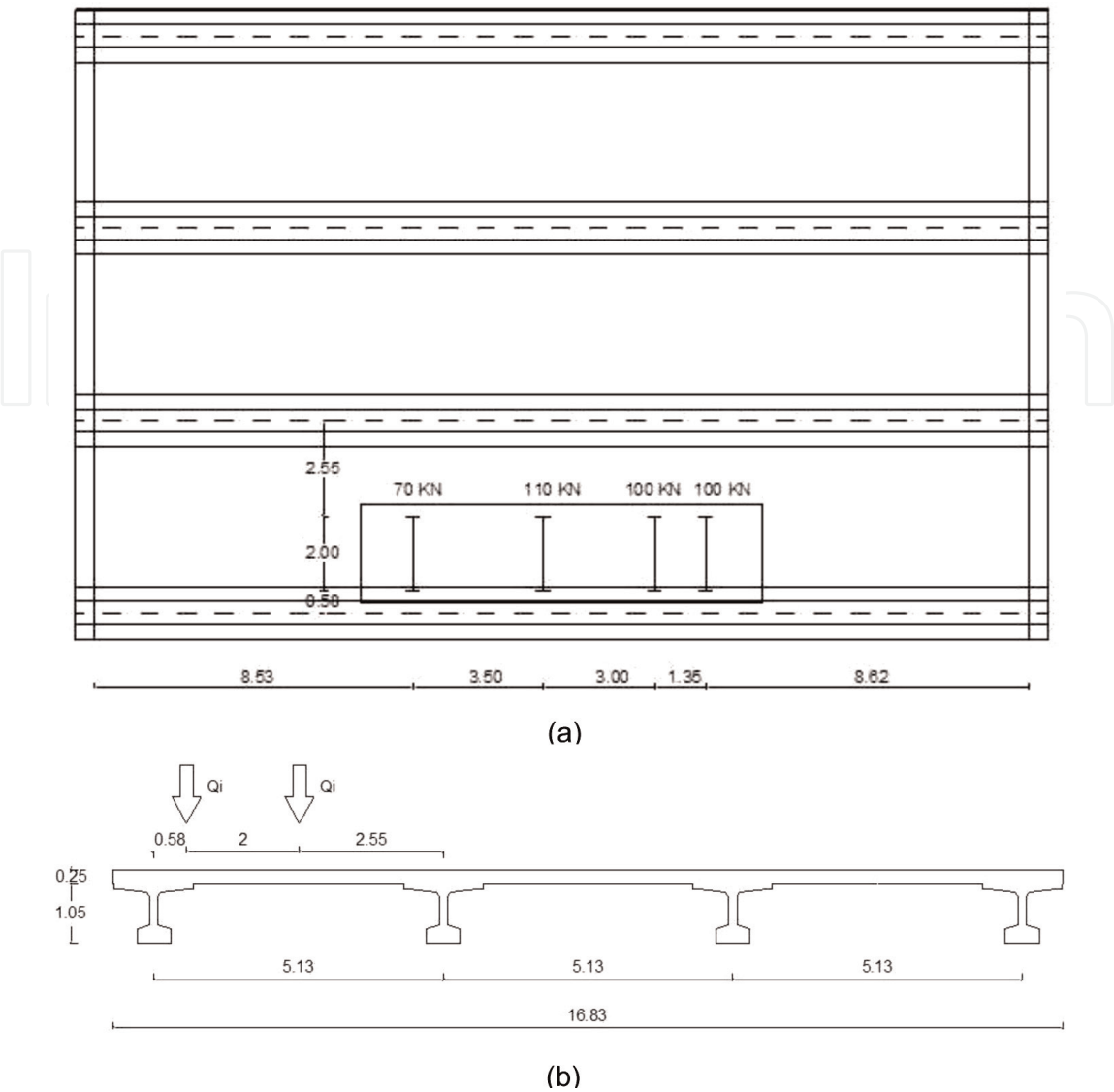


Figure 8.
Load state generated by the actuation of a four-axle truck 70 + 110 + 100 + 100 kN: (a) plan view; (b) front view.

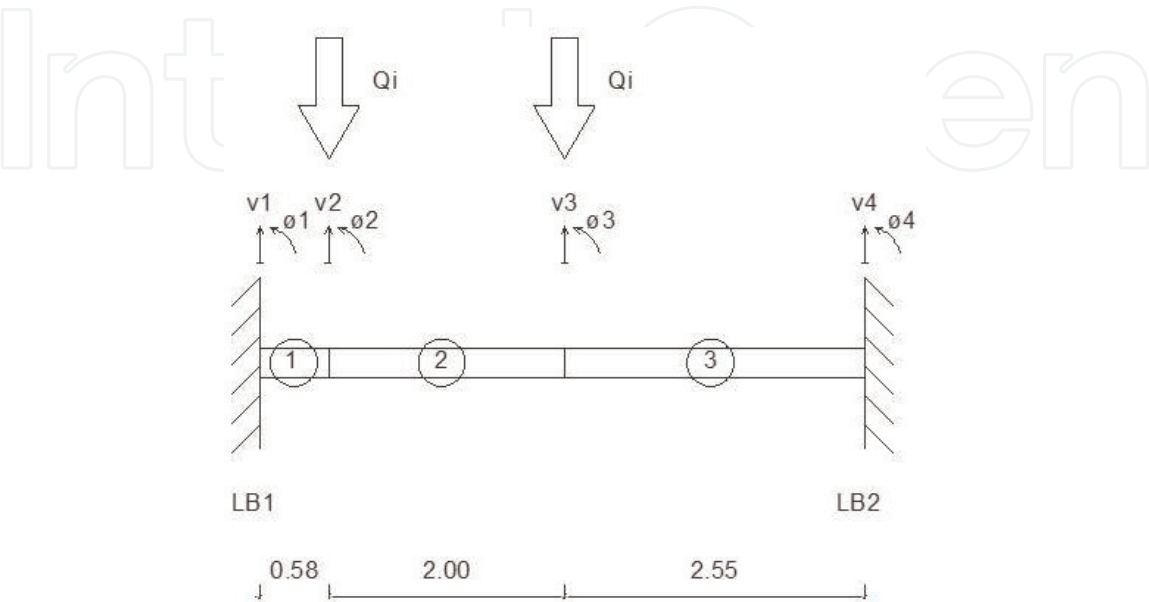


Figure 9.
Load state generated by the actuation of a four-axle truck. Rigid step.

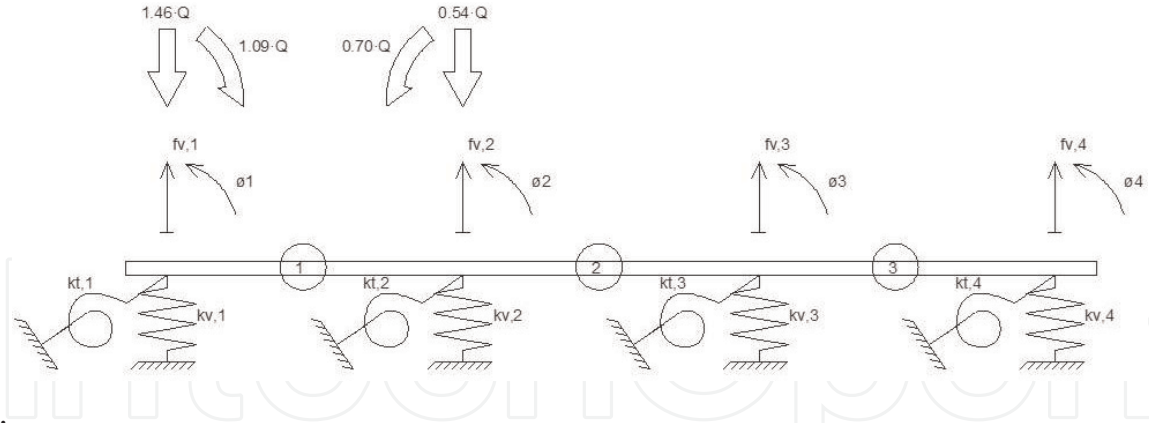


Figure 10.

Load state generated by the actuation of a four-axle truck. Flexible step.

Flexible step (**Figure 10**).

$$\begin{pmatrix} -1.46Q \\ -1.09Q \\ -0.54Q \\ 0.70Q \\ 0 \\ 0 \\ 0 \\ 0 \end{pmatrix} = \begin{pmatrix} & & & 0 & 0 & 0 & 0 \\ K_{11} + K_{B,end} & K_{12} & & 0 & 0 & 0 & 0 \\ K_{21} & K_{22} + K_{11} + K_{B,c} & & K_{12} & & 0 & 0 \\ & & & & & 0 & 0 \\ 0 & 0 & & & & & \\ & & K_{21} & & & & \\ 0 & 0 & & K_{22} + K_{11} + K_{B,c} & K_{12} & & \\ & & 0 & 0 & K_{21} & K_{22} + K_{B,end} & \\ 0 & 0 & 0 & 0 & & & \end{pmatrix} \cdot \begin{pmatrix} f_{v,1} \\ \theta_1 \\ f_{v,2} \\ \theta_2 \\ f_{v,3} \\ \theta_3 \\ f_{v,4} \\ \theta_4 \end{pmatrix}$$

Truck axle 1

Deflection in the center of the span of the longitudinal beams

$$f_{cl,Q(x),i} = f_{v,i} \cdot \sin\left(\frac{\pi \cdot x}{L}\right) = \begin{pmatrix} -2.39 \text{ mm} \\ -1.20 \text{ mm} \\ -0.21 \text{ mm} \\ 0.30 \text{ mm} \end{pmatrix}$$

Maximum bending moments

$$M_{fmax,n} = \frac{Q \cdot (L - x) \cdot x}{L} \cdot \frac{f_{v,n}}{\sum_{i=1}^N f_{v,i}} = \begin{pmatrix} 268 \text{ KN} \cdot \text{m} \\ 135 \text{ KN} \cdot \text{m} \\ 24 \text{ KN} \cdot \text{m} \\ -34 \text{ KN} \cdot \text{m} \end{pmatrix}$$

Maximum shear forces

$$Q_{max,n} = \frac{Q \cdot (L - x)}{L} \cdot \frac{f_{v,n}}{\sum_{i=1}^N f_{v,i}} = \begin{pmatrix} 31 \text{ KN} \\ 16 \text{ KN} \\ 3 \text{ KN} \\ -4 \text{ KN} \end{pmatrix}$$

Truck axle 2

Deflection in the center of the spam of the longitudinal beams

$$f_{cl,Q(x),i} = f_{v,i} \cdot \sin\left(\frac{\pi \cdot x}{L}\right) = \begin{pmatrix} -4.27 \text{ mm} \\ -2.15 \text{ mm} \\ -0.38 \text{ mm} \\ 0.53 \text{ mm} \end{pmatrix}$$

Maximum bending moments

$$M_{fmax,n} = \frac{Q \cdot (L - x) \cdot x}{L} \cdot \frac{f_{v,n}}{\sum_{i=1}^N f_{v,i}} = \begin{pmatrix} 468 \text{ KN} \cdot \text{m} \\ 236 \text{ KN} \cdot \text{m} \\ 41 \text{ KN} \cdot \text{m} \\ -59 \text{ KN} \cdot \text{m} \end{pmatrix}$$

Maximum shear forces

$$Q_{max,n} = \frac{Q \cdot (L - x)}{L} \cdot \frac{f_{v,n}}{\sum_{i=1}^N f_{v,i}} = \begin{pmatrix} 39 \text{ KN} \\ 20 \text{ KN} \\ 3 \text{ KN} \\ -5 \text{ KN} \end{pmatrix}$$

Truck axle 3

Deflection in the center of the spam of the longitudinal beams

$$f_{cl,Q(x),i} = f_{v,i} \cdot \sin\left(\frac{\pi \cdot x}{L}\right) = \begin{pmatrix} -3.69 \text{ mm} \\ -1.86 \text{ mm} \\ -0.33 \text{ mm} \\ 0.46 \text{ mm} \end{pmatrix}$$

Maximum bending moments

$$M_{fmax,n} = \frac{Q \cdot (L - x) \cdot x}{L} \cdot \frac{f_{v,n}}{\sum_{i=1}^N f_{v,i}} = \begin{pmatrix} 409 \text{ KN} \cdot \text{m} \\ 206 \text{ KN} \cdot \text{m} \\ 36 \text{ KN} \cdot \text{m} \\ -51 \text{ KN} \cdot \text{m} \end{pmatrix}$$

Maximum shear forces

$$Q_{max,n} = \frac{Q \cdot (L - x)}{L} \cdot \frac{f_{v,n}}{\sum_{i=1}^N f_{v,i}} = \begin{pmatrix} 41 \text{ KN} \\ 21 \text{ KN} \\ 4 \text{ KN} \\ -5 \text{ KN} \end{pmatrix}$$

Truck axle 4

Deflection in the center of the spam of the longitudinal beams

$$f_{cl,Q(x),i} = f_{v,i} \cdot \sin\left(\frac{\pi \cdot x}{L}\right) = \begin{pmatrix} -3.43 \text{ mm} \\ -1.73 \text{ mm} \\ -0.30 \text{ mm} \\ 0.43 \text{ mm} \end{pmatrix}$$

Maximum bending moments

$$M_{fmax,n} = \frac{Q \cdot (L - x) \cdot x}{L} \cdot \frac{f_{v,n}}{\sum_{i=1}^N f_{v,i}} = \begin{pmatrix} 385 \text{ KN} \cdot \text{m} \\ 194 \text{ KN} \cdot \text{m} \\ 34 \text{ KN} \cdot \text{m} \\ -48 \text{ KN} \cdot \text{m} \end{pmatrix}$$

Maximum shear forces

$$Q_{max,n} = \frac{Q \cdot (L - x)}{L} \cdot \frac{f_{v,n}}{\sum_{i=1}^N f_{v,i}} = \begin{pmatrix} 45 \text{ KN} \\ 22 \text{ KN} \\ 4 \text{ KN} \\ -6 \text{ KN} \end{pmatrix}$$

Deflection and efforts generated by the action of the four-axle truck

$$f_{v,i} = \begin{pmatrix} -13.78 \text{ mm} \\ -6.94 \text{ mm} \\ -1.22 \text{ mm} \\ 1.72 \text{ mm} \end{pmatrix}$$

$$M_{fmax,i} = \begin{pmatrix} 1,323 \text{ KN} \cdot \text{m} \\ 667 \text{ KN} \cdot \text{m} \\ 117 \text{ KN} \cdot \text{m} \\ -165 \text{ KN} \cdot \text{m} \end{pmatrix}$$

$$Q_{max,i} = \begin{pmatrix} 138 \text{ KN} \\ 70 \text{ KN} \\ 12 \text{ KN} \\ -17 \text{ KN} \end{pmatrix}$$

4. Conclusions

The proposed method for the analysis of the cross-sectional distribution of live loads on girder bridge decks allows determining the cross-sectional distribution in

different configurations of girder bridge decks without the need to resort to complex calculation models that involve depth computing power and excessive analysis time. The method is also applicable for modern synthetic materials, such plastic composites, self-repair. The simplicity of the method allows an easy integration into optimal bridge design strategies [28] or more heuristic approaches [29–33] to challenge today's competitive world intelligently.

Acknowledgements

This work has received funding from the European's Union Horizon 2020 research and innovation program under the grant agreement No 769373 (FORESEE project). This paper reflects only the author's views. The European Commission and INEA are not responsible for any use that may be made of the information contained therein.

Author details


Alvaro Gaute-Alonso^{1*} and David Garcia-Sanchez²

1 Group of Research and Civil Engineering Dynamic Analysis, University of Cantabria "GiaDe", Santander, Spain

2 TECNALIA Basque Research and Technology, Alliance "BRTA", Derio, Spain

*Address all correspondence to: alvaro.gaute@unican.es

IntechOpen

© 2022 The Author(s). Licensee IntechOpen. This chapter is distributed under the terms of the Creative Commons Attribution License (<http://creativecommons.org/licenses/by/3.0>), which permits unrestricted use, distribution, and reproduction in any medium, provided the original work is properly cited. 

References

- [1] Ahsan R, Rana S, Sayeed Nurul G. Cost optimum design of posttensioned I-girder bridge using global optimization algorithm. *Journal of Structural Engineering*. 2012;**138**(2):273-284. DOI: 10.1061/(ASCE)ST.1943-541X.0000458
- [2] Douthe C, Caron J, Baverel O. Gridshell structures in glass fibre reinforced polymers. *Construction and Building Materials*. 2010;**24**(9): 1580-1589. DOI: 10.1016/j.conbuildmat.2010.02.037
- [3] Peloux LD, Tayeb F, Lefevre B, Baverel O, Caron J-F. Formulation of a 4-DoF torsion/bending element for the formfinding of elastic gridshells. Amsterdam: Proceedings of the International Association for Shell and Spatial Structures (IASS) Symposium; 2015
- [4] Rombouts J, Lombaert G, Laet LD, Schevenels M. A novel shape optimization approach for strained gridshells: Design and construction of a simply supported gridshell. *Engineering Structures*. 2019;**192**:166-180. DOI: 10.1016/j.engstruct.2019.04.101
- [5] D. Veenendaal and. P. Block. An overview and comparison of structural form finding methods for general networks. *International Journal of Solids and Structures*. 2012;**49**: 3741-3753. DOI: 10.1016/j.ijsolstr.2012.08.008
- [6] Samartin Quiroga A. Notas al cálculo de esfuerzos en tableros de puentes. *Hormigón y Acero*. 1971;**22**(98):115-135
- [7] Manterola J. Cálculo de tableros por el método del emparrillado. *Hormigón y Acero*. 1977;**28**(122):93-149
- [8] Jing-xian S. Application of T-beam Grillage model in reconstruction design of dangerous bridge. 4th International Conference on Mechanical, Control and Computer Engineering (ICMCCE); 2019. DOI: 10.1109/ICMCCE48743.2019.00190
- [9] Zhou Y, Ji Y. Comparison and Analysis of the Results of Grillage Method and Single Beam Method to Continuous Box Girder with Variable Width. Banff, Canada: 4th International Conference on Transportation Information and Safety (ICTIS); 2017
- [10] Feng JP, Zhang XL, Zhu Z, Huang PM, Wang D, Niu YW. Application on Grillage Method in Box Girder Bridges. *Applied Mechanics and Materials*. 2013;**1**:886-890. DOI: 10.4028/www.scientific.net/amm.438-439.886
- [11] Dicleli M, Erhan S. Live Load Distribution Formulas for Single-Span Prestressed Concrete Integral Abutment Bridge Girders. *Journal of Bridge Engineering*. 2009;**14**:6. DOI: 10.1061/(ASCE)BE.1943-5592.0000007
- [12] Fu CC, Elhelbawey M, Sahin MA, Schelling DR. Lateral distribution factor from bridge field testing. *Journal of Structural Engineering*. 1996;**122**(9): 1106-1109. DOI: 10.1061/(ASCE)0733-9445(1996)122:9(1106)
- [13] Gheitasi A, Harris DK. Overload flexural distribution behavior of composite steel girder bridges. *Journal of Bridge Engineering*. 2015;**20**(5) 04014076:1-15. DOI: 10.1061/(ASCE)BE.1943-5592.0000671
- [14] Hess S, Filosa F, Ross BE, Cousins TE. Live Load Testing of NEXT-D Bridges to Determine

- Distribution Factors for Moment. *Journal of Performance of Constructed Facilities*. 2020;**34**(4) 04020063:1-9. DOI: 10.1061/(ASCE)CF.1943-5509.0001452
- [15] J. Huang and. J. Davis. Live load distribution factors for moment in NEXT beam bridges. *Journal of Bridge Engineering*. 2018;**23**(3). 06017010:1-7. DOI: 10.1061/(ASCE)BE.1943-5592.0001202
- [16] Huo XS, Wasserman EP, Zhu P. Simplified method of lateral distribution of live load moment. *Journal of Bridge Engineering*. 2004;**9**(4):382-390. DOI: 10.1061/(ASCE)1084-0702(2004)9:4(382)
- [17] Idriss RL, Liang Z. In-service shear and moment girder distribution factors in simple-span prestressed concrete girder bridge. *Journal of the Transportation Research Board*. 2010; **2172**:142-150. DOI: 10.3141/2172-16
- [18] Kim YJ, Tanovic R, Wight G. Load configuration and lateral distribution of NATO wheeled military trucks for steel I-girder bridges. *Journal of Bridge Engineering*. 2010;**15**(6):740-748. DOI: 10.1061/(ASCE)BE.1943-5592.0000113
- [19] Semendary AA, Steinberg EP, Walsh KK, Barnard E. Live-load moment-distribution factors for an adjacent precast prestressed concrete box beam bridge with reinforced UHPC shear key connections. *Journal of Bridge Engineering*. 2017;**22**(11):04017088/1-04017088/18
- [20] Yalcin OF, Diclel M. Comparative study on the effect of number of girders on live load distribution in integral abutment and simply supported bridge girders. *Advances in Structural Engineering*. 2013;**16**(6):1011-1034. DOI: 10.1260/1369-4332.16.6.1011
- [21] Harris DK. Assessment of flexural lateral load distribution methodologies for stringer bridges. *Engineering Structures*. 2010;**32**(11):3443-3451. DOI: 10.1016/j.engstruct.2010.06.008
- [22] Kong S, Zhuang L, Tao M, Fan J. Load distribution factor for moment of composite bridges with multi-boxgirders. *Engineering Structures*. 2020;**215**(110716):1-19. DOI: 10.1016/j.engstruct.2020.110716
- [23] Terzioglu T, Hueste MBD, Mande JB. Live Load Distribution Factors for Spread Slab Beam Bridges. *Journal of Bridge Engineering*. 2017;**22**(10) 04017067:1-15. DOI: 10.1061/(ASCE)BE.1943-5592.0001100
- [24] G. o. S. Ministry of Public Works. 18.2.1. Ancho eficaz del ala en piezas lineales. EHE - 08. Instrucción de Hormigón Estructural; 2011
- [25] G. o. S. Ministry of Public Works. 4.5. Anchura eficaz elástica. RPX-95. Recomendaciones para el proyecto de puentes mixtos para carreteras; 1996
- [26] American Association of State Highway and Transportation Officials. Standard specifications for highway bridges. 1st ed. Washington, DC; 1931
- [27] Baker WF, Beghini LL, Mazurek A, Carrion J, Beghini A. Maxwell's reciprocal diagrams and discrete Michell frames. *Structural and Multidisciplinary Optimization*. 2013;**48**(2):267-277. DOI: 10.1007/s00158-013-0910-0
- [28] Kuang Y, Ou J. Self-repairing performance of concrete beams strengthened using superelastic SMA wires in combination with adhesives released from hollow fibers. *Smart*

Materials and Structures. 2008;**17**.
DOI: 10.1088/0964-1726/17/2/025020

[29] Ghani SN. Performance of global optimization algorithm EOP for non-linear non-differentiable constrained objective functions. New York: Proceedings of IEEE International Conference on Evolutionary Computation; 1995

[30] Ghani S. A versatile algorithm for optimization of a nonlinear non-differentiable constrained objective function. UKAEA Harwell. R-13714. HMSO Publications Centre; 1989

[31] Hassanain MA, Loov RE. Cost optimization of concrete bridge infrastructure. Canadian Journal of Civil Engineering. 2003;**30**(5):841-843.
DOI: 10.1139/L03-045

[32] Jones H. Minimum cost prestressed concrete beam design. Journal of Structural Engineering. 1985;**111**:11.
DOI: 10.1061/(ASCE)0733-9445(1985)111:11(2464)

[33] Lounis Z, Cohn MZ. Optimization of precast prestressed concrete bridge beam systems. Precast/Prestressed Concrete Institute Journal. 1993;**38**(4):60-78.
DOI: 10.15554/pcij.07011993.60.78